Eur Radiol (2015) 25:1392–1398
DOI 10.1007/s00330-014-3542-x

CONTRAST MEDIA

Assessing liver function in patients with HBV-related HCC: a comparison of T_1 mapping on Gd-EOB-DTPA-enhanced MR imaging with DWI

Ying Ding · Sheng-Xiang Rao · Caizhong Chen · Renchen Li · Meng-Su Zeng

Received: 10 September 2014 / Accepted: 21 November 2014 / Published online: 19 December 2014
© European Society of Radiology 2014

Abstract
Objectives To compare the potential of T_1 mapping on gadoxetic acid (Gd-EOB-DTPA)-enhanced magnetic resonance imaging (MRI) and diffusion-weighted imaging (DWI) for assessing liver function in patients with hepatitis B virus (HBV)-related hepatocellular carcinoma (HCC).
Methods One hundred consecutive patients with known HBV-related HCCs were included. T_1 relaxation time and apparent diffusion coefficient (ADC) of the liver were measured, and the reduction rate of T_1 relaxation time (Δ%) was calculated. T_1 relaxation time measurements were compared with ADC values according to the Model for End-Stage Liver Disease (MELD) score.
Results Hepatobiliary phase (HBP) and Δ% of T_1 relaxation time measurements showed significant correlations with MELD score (rho=0.571, $p<0.0001$; rho=−0.573, $p<0.0001$, respectively). HBP and Δ% of T_1 relaxation time were significantly different between good (MELD ≤8) and poor liver function (MELD ≥9) ($p<0.0001$ for both). Areas under the receiver operating characteristic curves (AUCs) of T_1 relaxation time for HBP (AUC 0.84) and Δ% (AUC 0.82) were significantly better than for ADC (AUC 0.53; $p<0.0001$).
Conclusions T_1 mapping on Gd-EOB-DTPA-enhanced MRI showed promise for evaluating liver function in patients with HBV-related HCC, while DWI was not reliable. HBP T_1 relaxation time measurement was equally accurate as Δ% measurement.
Key Points
- *T_1 mapping on Gd-EOB-DTPA MRI was accurate for assessing liver function.*
- *HBP T_1 relaxation time measurement was as accurate as Δ% T_1*
- *T_1 mapping on Gd-EOB-DTPA MRI was more accurate than DWI-ADC measurement.*

Keywords Gd-EOB-DTPA · T_1 relaxation time · Magnetic resonance imaging · Diffusion-weighted imaging · Liver function

Y. Ding · S.-X. Rao (✉) · C. Chen · R. Li · M.-S. Zeng
Department of Radiology, Zhongshan Hospital of Fudan University, 180 Fenglin RoadXuhui District Shanghai, China 200032
e-mail: raoxray@163.com

Y. Ding
e-mail: ding.ying@zs-hospital.sh.cn

C. Chen
e-mail: chen.caizhong@126.com

R. Li
e-mail: li.renchen@126.com

M.-S. Zeng
e-mail: zengmengsu@gmail.com

Introduction

The evaluation of liver functional reserve is important in selecting the appropriate patients for partial hepatectomy or ablation of hepatic tumours. Liver failure is the major cause of mortality after liver resection, especially in patients with chronic liver disease or cirrhosis. It is important to assess both total and segmental liver function before liver surgery in order to predict the remnant liver functional reserve. In clinical practice, liver function tests include the indocyanine green (ICG) clearance rate at 15 minutes [1], computed tomography volumetry [2], and clinical scoring systems such as the Child-Pugh or Model for End-Stage Liver Disease (MELD) scores [3–5]. However, these methods offer only global assessment of liver function, which cannot assess the heterogeneous functional distribution in the liver. A tool that would enable us to estimate segmental liver functional reserve prior to surgery

would be beneficial, as it could facilitate a more risk-adapted treatment strategy.

Diffusion-weighted imaging (DWI) and magnetic resonance imaging (MRI) using gadoxetic acid (Gd-EOB-DTPA) have recently shown promise for the evaluation of segmental liver functional reserve [6–11]. DWI is based on the random Brownian motion of water molecules within the voxel. Changes in hepatic diffusion are indicative of tissue changes on a cellular level, and may be used to assess liver function through the use of apparent diffusion coefficient (ADC) mapping. A previous study showed that ADC values could reflect underlying cellular swelling and damage, which may be useful for identifying patients at risk of hepatocellular impairment from biliary obstruction [6]. However, Kim et al. [12] reported that DWI-ADC was not suitable for predicting postoperative hepatic insufficiency, advanced liver fibrosis, or cirrhosis in patients with hepatitis B virus (HBV)-related hepatocellular carcinoma (HCC). Gd-EOB-DTPA is taken up by hepatocytes and secreted into the biliary system, and this pathway is similar to those for ICG. Previous studies have shown that patients with liver dysfunction presented with decreased liver parenchymal enhancement on Gd-EOB-DTPA-enhanced hepatobiliary-phase (HBP) MR imaging using direct measurement of liver parenchymal signal intensity [7–9] or calculation of perfusion parameters [10, 11]. The clinical applicability of this method of measurement, however, is challenging due to the nonlinear relationship between the MR signal intensity and gadolinium concentration and the variations caused by various technical factors [13]. Perfusion imaging has limited availability in light of the lack of standardized acquisition techniques, complex mathematical modelling, and motion artefacts induced by breathing motions during image acquisition.

An alternative approach to the direct measurement of signal intensity and perfusion imaging is to evaluate the T_1 relaxation time of the liver parenchyma, which in theory is directly correlated with the concentration of Gd-EOB-DTPA. Our previous study showed that Gd-EOB-DTPA-enhanced MR imaging was useful for evaluating non-alcoholic fatty liver disease in an animal model by measuring T_1 relaxation time [14]. Studies have also demonstrated that Gd-EOB-DTPA-enhanced MR imaging using T_1 mapping can be helpful for estimating liver function according to the Child-Pugh score in patients with chronic liver disease or cirrhosis [15, 16]. In clinical practice, the MELD score could be used for the selection of patients for surgery or liver transplantation, as well as for determining optimal treatment for patients with hepatocellular carcinoma (HCC) [5]. Several authors have suggested that hepatic resection for HCC could be carried out safely in patients with cirrhosis who have a MELD score of less than 8 [4, 5].

In order to determine whether Gd-EOB-DTPA-enhanced MR imaging using T_1 mapping can be used to predict the remnant liver functional reserve after liver resection, we must first assess whether there are any differences in T_1 relaxation time of the liver parenchyma among patients with different MELD scores. Hence, our aim was to evaluate whether there were correlations between the T_1 relaxation time of the liver parenchyma and the MELD score and to compare the results of T_1 relaxation time measurement with DWI-ADC measurement.

Materials and methods

Patients

This retrospective study was approved by the institutional review board of our hospital, and the requirement for informed consent was waived. We retrospectively evaluated 100 patients who were diagnosed with HCC at our institution between March 2011 and December 2013. Inclusion criteria consisted of the following: (a) availability of pre-treatment Gd-EOB-DTPA-enhanced MR imaging using T_1 mapping; (b) HCC diagnosed by pathology (surgery or biopsy), typical dynamic imaging studies, and alpha fetoprotein serology, according to the American Association for the Study of Liver Diseases (AASLD) guidelines [17]; (c) chronic viral hepatitis B infection [hepatitis B surface antigen (+)]; (d) no previous oncologic treatment or liver resection; (e) no tumour invasion of branches and trunk of the portal vein or hepatic veins on MR images; and (f) no other diffuse liver disease (primary sclerosing cholangitis, primary biliary cirrhosis, etc.).

Gd-EOB-DTPA-enhanced MR imaging and DWI

MR imaging was carried out on a 1.5 T MR system with a phased-array coil (MAGNETOM Aera; Siemens Medical Solution, Erlangen, Germany). For T_1 mapping with *syngo* MapIt, a dual flip-angle 3D gradient-echo sequence with volumetric interpolated breath-hold examination (VIBE) was performed before and after injection of Gd-EOB-DTPA (Primovist®; Bayer-Schering Pharma AG, Berlin, Germany). The parameters were as follows: repetition time (TR), 4.38 milliseconds (ms); echo time (TE), 1.93 ms; flip angle, 2° and 12°; field of view (FOV), 380–400×300–324 mm; matrix, 216×288; and 20-cm slab thickness, resulting in an interpolated 5-mm section thickness. A parallel imaging technique (R=2) was performed using generalized autocalibrating partially parallel acquisition (GAPPA). In all patients, 0.025 mmol/kg body weight of Gd-EOB-DTPA was injected manually at a rate of approximately 1 ml/sec, as recommended, by one investigator through a 20-gauge intravenous catheter placed in a cubical or cephalic vein. Immediately afterwards, a 20 ml saline flush was injected at the same injection

rate. T_1 mapping for HBP was obtained before and at 20 minutes after Gd-EOB-DTPA administration.

Three scan trace free-breathing DW images were obtained prior to Gd-EOB-DTPA injection using a single-shot spin-echo planar imaging sequence (TR/TE, 3,200/56 ms; slice thickness, 5.5 mm; matrix size, 84×128; FOV, 380–400×300–324 mm), with B-values of 0 and 500 s/mm^2. A parallel imaging technique (R=2) was performed using GAPPA.

Image evaluation

Quantitative T_1 relaxation time maps and ADC maps were derived automatically on a voxel-by-voxel basis. The MR data sets were transferred to a workstation (Leonardo, Siemens, Erlangen, Germany) to measure the T_1 relaxation time and ADC value of the liver parenchyma using operator-defined regions of interest (ROIs). We manually drew the ROIs covering the whole right lobe of liver on the same mid-liver slice of T_1-weighted images and high-B-value (B=500 s/mm^2) DW images, except for the border of the liver (to avoid partial volume effects), any visible lesions, major hepatic veins, and the inferior vena cava, and then copied to corresponding T_1 maps and ADC maps (Fig. 1a–d). All MR images were evaluated by a single reader (Meng-su Zeng) with five years of experience in reading abdominal MR images, who was blinded to clinical results. In addition, the reduction rate of T_1 relaxation time between pre-contrast and HBP was calculated, as follows: reduction rate (Δ%)=100×(T_{1pre}-T_{1post})/T_{1pre}, where T_{1pre} and T_{1post} were the T_1 relaxation times of the liver before and after Gd-EOB-DTPA injection.

MELD score

MELD incorporates three widely available laboratory variables—serum bilirubin, serum creatinine, and the international normalized ratio for prothrombin time (INR)—to predict global liver function. It is calculated according to the following formula [5]: MELD=3.78[Ln serum bilirubin (mg/dL)]+11.2[Ln INR]+9.57[Ln serum creatinine (mg/dL)]+6.43. To prevent the occurrence of scores below 0, any value less than 1 is given a value of 1. The global liver function of each patient was categorized as either good (MELD ≤8) or poor (MELD ≥9).

Statistical analysis

Statistical analyses were performed using MedCalc (MedCalc for Windows version 11.5.0.0, www.medcalc.be). The correlation between MR measurements (ADC and pre-, post-, and Δ% measurements of T_1 relaxation time) and MELD scores was assessed using Spearman's rank-order correlation test and correlation coefficients (rho). The ADC and pre- ,post-, and Δ% measurements of T_1 relaxation time were compared between good liver function and poor liver function using the student's *t* test when normally distributed and the Mann–Whitney *U* test when not normally distributed. A paired-samples *t* test or Wilcoxon test (when not normally distributed) were used to compare the pre- and post-T_1

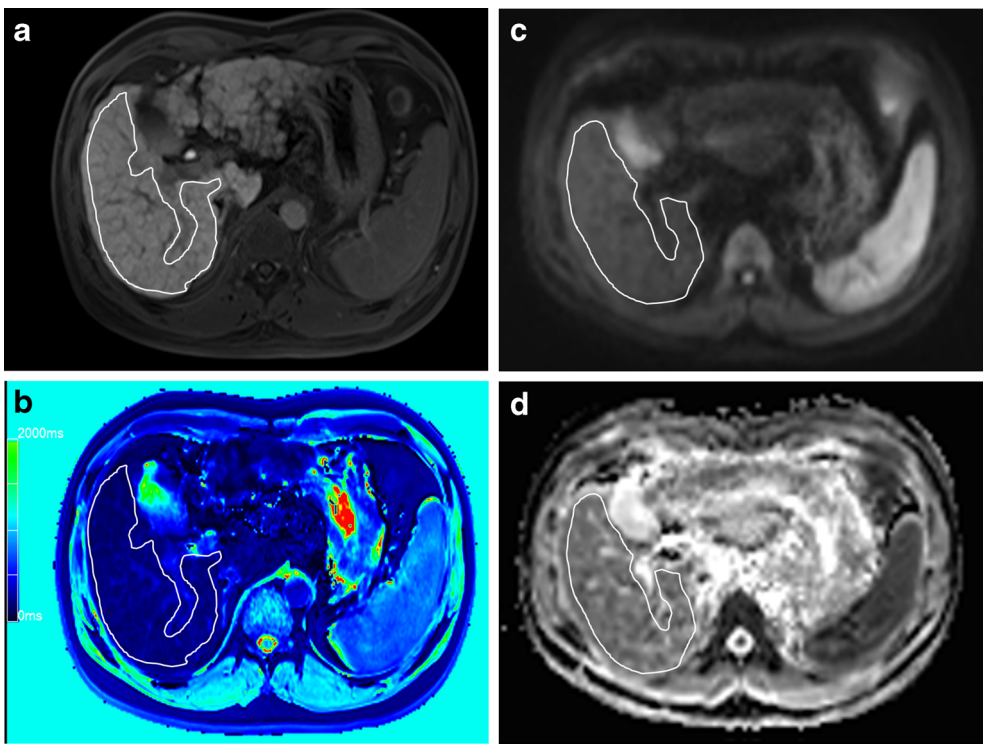


Fig. 1 a–d Examples of placement of regions of interest (ROIs) in the same area of the liver parenchyma on a hepatobiliary phase image (*a*) and corresponding T_1 map to measure the T_1 relaxation time (*b*), and on high-b-value diffusion-weighted (DW) images (*c*) and corresponding apparent diffusion coefficient (ADC) maps (*d*)

relaxation time measurements, respectively, between good and poor liver function. In addition, receiver operating characteristic (ROC) analyses were constructed to determine the potential diagnostic performance for differentiating patients with good liver function from those with poor function. Corresponding areas under the ROC curve (AUCs), sensitivities, specificities, positive likelihood ratio (+LR), and negative likelihood ratio (−LR) were calculated with a 95 % confidence interval (CI). Differences in diagnostic performance were analyzed by comparing the ROC curves. Differences with a p value smaller than 0.05 were considered statistically significant.

Results

Baseline patient characteristics

A total of 100 patients (68 men and 32 women; median age, 56 years; range, 30–76 years) meeting all of the criteria were included in the study. Sixty-one patients underwent partial hepatectomy and 39 underwent percutaneous radiofrequency ablation (RFA) for HCC. There were 167 lesions in 100 patients, and 79 lesions were resected. The diameters among all lesions ranged from 0.8 cm to 5.5 cm. The numbers of lesion locations in each of the segments from I to VIII were 7, 21, 25, 20, 37, 23, 21, and 13, respectively. Sixty-eight patients were classified as having good liver function (MELD score ≤8) and 32 were classified as having poor liver function (MELD score ≥9). The median length of time between Gd-EOB-DTPA-enhanced MR imaging and laboratory testing was two days (range, 1–5 days).The main patient characteristics are summarized in Table 1.

MR measurements and MELD score

Table 2 shows the relationships between T_1 relaxation time measurements or ADC values and MELD scores. HBP T_1 relaxation time (rho=0.571, $p<0.0001$) and Δ% of T_1 relaxation time (rho=−0.573, $p<0.0001$) showed significant correlations with MELD scores, while pre-contrast and ADC values did not correlate significantly with MELD scores (rho=0.100, $p=0.32$; rho=−0.021, $p=0.84$, respectively).

Table 2 Correlations between the MELD scores and T_1 relaxation time, ADC value

	rho	95 % CI	p
T_1 relaxation time			
Pre-contrast	0.100	−0.0983~0.291	0.32
Post-contrast	0.571	0.412~0.690	<0.0001
Reduction rate (Δ%)	−0.573	−0.691~−0.424	<0.0001
ADC (10^{-3} mm^2/s)	−0.021	−0.217~0.176	0.84

ADC apparent diffusion coefficient, *MELD* Model for End-Stage Liver Disease

The mean values for the T_1 relaxation time measurements (pre/post-contrast and Δ%) are provided in Table 3. The T_1 relaxation time decreased significantly after administration of Gd-EOB-DTPA, from a mean of 723.6 ms to 217.3 ms with good liver function ($p<0.0001$) and from a mean of 755.8 ms to 292.3 ms with poor liver function ($p<0.0001$). There was no significant difference in pre-contrast T_1 relaxation time or ADC values between good and poor liver function ($p=0.14$ and $p=0.50$, respectively). The mean value of T_1 relaxation time increased and Δ% T_1 relaxation time decreased significantly on HBP with poor liver function ($p<0.0001$ for both)

Diagnostic performance for assessment of poor liver function

The ROC curves performed to compare the diagnostic performance of pre- and post-contrast and Δ% T_1 relaxation times for assessment of poor liver function (MELD score ≥9) are shown in Fig. 2. The corresponding sensitivity, specificity, + LR, and –LR values were provided in Table 4. The HBP (AUC 0.84) and Δ% T_1 relaxation times (AUC 0.82) were significantly better than pre-contrast T_1 relaxation times (AUC 0.59; $p<0.0001$ and $p=0.0022$, respectively) and

Table 1 Baseline characteristics of patients with hepatitis B virus-related hepatocellular carcinoma

	All	MELD score	
		≤8	≥9
Number (n)	100	68	32
Age (years), median (range)	56 (30–76)	54 (30–76)	58.5 (40–71)
Male/Female, n	68/32	58/10	10/22
MELD score, median (range)	8 (6–17)	7 (6–8)	10 (9–17)
ALT, median (range), IU/L	34.5 (11–665)	28.5 (11–211)	38.5 (14–665)
AST, median (range), IU/L	33.5 (13–1302)	30 (13–232)	47.5 (15–1302)

MELD Model for End-Stage Liver Disease, *ALT* alanine aminotransferase, *AST* aspartate aminotransferase

Table 3 Mean values (± standard deviation) of T_1 relaxation time (ms) and ADC (10^{-3} mm/s^2) value of the liver parenchyma

	All (n=100)	MELD score		p value
		≤8 (n=68)	≥9 (n=32)	
T_1 relaxation time				
Pre-contrast	733.9±100.8	723.6±102.5	755.8±94.9	0.14
Post-contrast	241.3±65.0	217.3±52.9	292.3±59.2	<0.0001
Reduction rate (Δ%)	67.1 %±7.6 %	69.9 %±6.1 %	61.2 %±7.1 %	<0.0001
ADC (10^{-3} mm^2/s)	1.42±0.15	1.43±0.16	1.41±0.14	0.50

ADC apparent diffusion coefficient, *MELD* Model for End-Stage Liver Disease

ADC values (AUC 0.53; p<0.0001 and p=0.0001, respectively). The difference in AUC between HBP and Δ% T_1 relaxation time was not significant (p=0.39).

Discussion

Our results indicated that HBP and Δ% T_1 relaxation time measurements on Gd-EOB-DTPA-enhanced MR imaging were significantly correlated with MELD scores and that AUCs for the assessment of poor liver function (MELD score ≥9) for HBP and Δ% T_1 relaxation time (AUC 0.84 and 0.82, respectively) were significantly higher than that for DWI (AUC 0.53). The HBP T_1 relaxation time was equal to the Δ% T_1 relaxation time in diagnostic performance. Neither pre-contrast T_1 relaxation time nor DWI-ADC were reliable in predicting liver function.

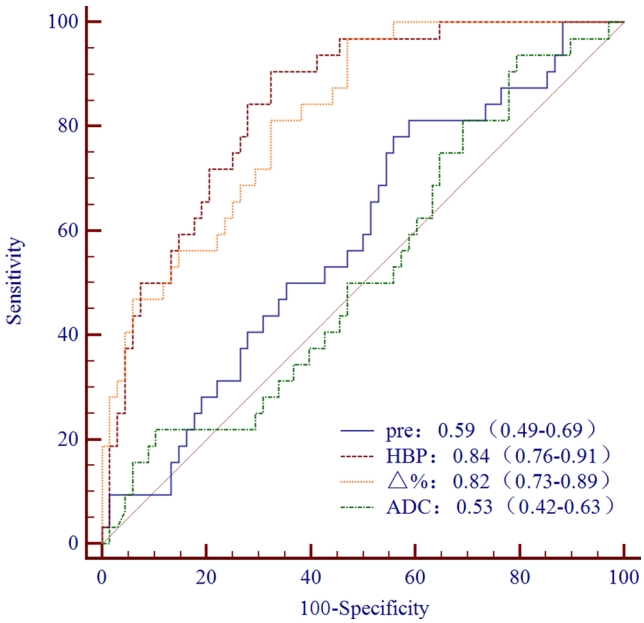


Fig. 2 Receiver operating characteristic (ROC) and area under the curve (AUC) for prediction of poor liver function using T_1 relaxation time and ADC. Numbers in parentheses represent 95 % confidence intervals. *Pre* pre-contrast phase, *HBP* hepatobiliary phase, Δ% reduction rate, *ADC* apparent diffusion coefficient

Most studies have shown that DWI after Gd-EOB-DTPA administration was feasible for the diagnosis of focal hepatic lesions. However, there is no consensus on the effect of Gd-EOB-DTPA administration on the ADC value of liver parenchyma [18–20]. Saito [18] et al. reported that Gd-EOB-DTPA had little effect on the ADC values of the liver, while other studies have shown that the ADC value was significantly reduced after enhancement, possibly due to the T2*-shortening effect of Gd-EOB-DTPA [19, 20]. In our department, therefore, we routinely perform the DWI before the injection of Gd-EOB-DTPA. Our poor results with DWI-ADC for the assessment of liver function were in keeping with those in a study by Kim et al. [12]. They reported that ADC values were not predictive of postoperative insufficiency in liver function, including persistent hyperbilirubinemia (total bilirubin level >5 mg/dl for more than five days after surgery) and postoperative death, in the absence of other causes in patients with HBV-related HCC. However, Tam et al. [6] showed that lower segmental ADC values may be associated with abnormal liver function in patients with malignant biliary obstruction. This may have been largely due to the fact that the patients in their study suffered severe segmental liver dysfunction which was already depicted on high-B-value DW (segmental hyperintensity) and T_2-weighted images (dilatation of the bile duct). We posited that the ADC values might be insufficient to detect the subtle changes of abnormal liver function when there were no visible signal intensity changes on routine and high-B-value DW images. Watanabe et al. [7] demonstrated that Gd-EOB-DTPA-enhanced MR imaging was more reliable than DWI-ADC for staging hepatic fibrosis, which was consistent with our results showing that Gd-EOB-DTPA-enhanced MR imaging using T_1 mapping was significantly more accurate than DWI-ADC in evaluating liver function.

Gd-EOB-DTPA-enhanced MR imaging using T_1 mapping also appears to have the potential to estimate liver function in patients with HBV-related HCC. Higher HBP T_1 relaxation time and corresponding lower Δ% T_1 relaxation time have been associated with worse liver function. Gd-EOB-DTPA is a liver-specific magnetic resonance imaging contrast agent that has up to 50 % hepatobiliary excretion in the normal liver. The functioning hepatocyte uptake of Gd-EOB-DTPA occurs primarily via the organic anion transporter polypeptides and

Table 4 Diagnostic performance for T_1 relaxation time and ADC value in assessing MELD score ≥9 by receiver operating characteristic (ROC) analyses

	AUC	Sensitivity	Specificity	+LR	−LR	Cutoff
Pre	0.59	81.3	41.2	1.38	0.46	>689.2
95 % CI	0.49–0.69	63.6–92.8	29.4–53.8	1.0–1.9	0.2–1.0	
HBP	0.84	90.6	67.7	2.80	0.14	>229.5
95 % CI	0.76–0.91	75.0–98.0	55.2–78.5	2.3–3.4	0.04–0.4	
Δ%	0.82	81.3	67.7	2.51	0.28	≤0.666
95 % CI	0.73–0.89	63.6–92.8	55.2–78.5	2.0–3.2	0.1–0.6	
ADC	0.53	93.8	20.6	1.18	0.30	$\leq 1.60\times10^{-3}$
95 % CI	0.42–0.63	79.2–99.2	11.7–32.1	0.7–1.9	0.08–1.2	

ADC apparent diffusion coefficient, *MELD* Model for End-Stage Liver Disease, *AUC* area under the ROC curve, *+LR* Positive likelihood ratio, *−LR* Negative likelihood ratio, *Pre* pre-contrast phase, *HBP* hepatobiliary phase, Δ%: reduction rate

biliary excretion via multidrug resistance-associated proteins [21–24]. In theory, liver dysfunction (higher MELD scores) may result in a lower number of normal hepatocytes. This impairs the uptake of Gd-EOB-DTPA by hepatocytes, which leads to lower concentrations of gadolinium in the liver parenchyma on HBP. We believe that this is the reason for the correlation between higher HBP T_1 relaxation times of the liver parenchyma and higher MELD scores. Katsube et al. [15] reported that post-contrast T_1 relaxation times of the liver parenchyma using Gd-EOB-DTPA-enhanced MR were significantly prolonged, and that reduction rates were significantly lower for Child-Pugh class B compared to Child-Pugh class A chronic hepatitis and normal liver function. Haimerl et al. [16] also confirmed that T_1 relaxation times showed a constant significant increase from Child-Pugh class A to class C, and a constant decrease in the reduction rate of T_1 relaxation times in patients with cirrhosis.

T_1 relaxation time is an absolute value, and appears to be more reliable and less subjective than the direct hepatic signal intensity method to assess liver function [25]. The *syngo* MapIt tool enables rapid MRI sequencing with high resolution using 3D VIBE [26]. In our department, we include this sequence in routine liver MR imaging. We acknowledge that the AUCs for the assessment of poor liver function using the T_1 relaxation time of Gd-EOB-DTPA-enhanced MRI in our study were not very high (up to 0.84). Verloh et al. [8] reported that relative enhancement provided high performance (AUC 0.87) for assessing impaired liver function (MELD >10). It is possible that the MELD scores of the patients in our study were relatively low (median score, 8; range 6–17). Furthermore, the MR scanner that we used was a 1.5 T system, which has less enhancement effect of the contrast agent compared with a 3.0 T system [27]. A study by de Bazelaire et al. [28] demonstrated that the T_1 relaxation time for the liver parenchyma was about 38 % longer at 3.0 T than at 1.5 T.

Another interesting finding was that T_1 relaxation time on HBP only was equal in diagnostic performance to T_1 relaxation time reduction after administration of Gd-EOB-DTPA for evaluation of liver function, which was consistent with results from our previous study in the analysis of non-alcoholic fatty liver disease in an animal model [14]. Katsube et al. [15] reported that post-contrast T_1 relaxation time and the reduction rate of T_1 relaxation time at 18 minutes after injection of Gd-EOB-DTPA yielded similar accuracy (89.0 % and 84.6 %, respectively) for distinguishing Child-Pugh B liver cirrhosis from other groups (Child-Pugh A ,chronic hepatitis, and normal liver function). Haimerl et al. [16] showed similar AUCs for the two methods in differentiating groups of liver function according to Child-Pugh score. These results suggest that HBP T_1 relaxation time measurement may be sufficient and that calculating the reduction rate may not be necessary. This less time-consuming method is feasible in the context of busy daily clinical practice.

There were limitations in our study. Firstly, because of its retrospective nature, our study could not avoid sampling bias. Secondly, we compared MR measurements only with MELD scores, and did not assess other liver function tests such as ICG clearance. Previous studies have demonstrated that ICG clearance rates were well-correlated with liver enhancement on HBP [29, 30]. Few patients underwent ICG clearance testing in our study. Thirdly, we performed DWI using two B-values (0 and 500 sec/mm2), which may have affected the accuracy of the ADC measurements. Finally, we should have evaluated the correlation between the MR measurements and histological results. However, 39 patients in our study did not undergo liver tumour resection. In clinical practice, the MELD score has been proved to correctly estimate global liver functional reserve.

In conclusion, measurement of T_1 relaxation time on Gd-EOB-DTPA-enhanced MR imaging was accurate in evaluating liver function in patients with HBV-related HCC, which may be a biomarker for estimating the remnant liver functional reserve. ADC measurement was not reliable for the assessment of liver functional reserve. HBP T_1 relaxation time was equally accurate as evaluation of T_1 relaxation time reduction (Δ%). The next step, the correlation between separate liver

segments and pathology, should be validated in a prospective study with a large patient cohort.

Acknowledgments The scientific guarantor of this publication is Sheng-xiang Rao. The authors of this manuscript declare no relationships with any companies, whose products or services may be related to the subject matter of the article. This study has received funding by Project supported by the National Science Foundation of China (Grant No. 81371543). No complex statistical methods were necessary for this paper. Institutional Review Board approval was obtained. Written informed consent was waived by the Institutional Review Board. Methodology: case–control study, performed at one institution.

Project supported by the National Science Foundation of China (Grant No. 81371543)

References

1. Zipprich A, Kuss O, Rogowski S et al (2010) Incorporating indocyanin green clearance into the Model for End Stage Liver Disease (MELD-ICG) improves prognostic accuracy in intermediate to advanced cirrhosis. Gut 59:963–968
2. Zappa M, Dondero F, Sibert A, Vullierme MP, Belqhiti J, Vilqrain V (2009) Liver regeneration at day 7 after right hepatectomy: global and segmental volumetric analysis by using CT. Radiology 252:426–432
3. Stauber RE, Wagner D, Stadlbauer V et al (2009) Evaluation of indocyanine green clearance and model for end-stage liver disease for estimation of short-term prognosis in decompensated cirrhosis. Liver Int 29:1516–1520
4. Cucchetti A, Ercolani G, Vivarelli M et al (2006) Impact of model for end-stage liver disease (MELD) score on prognosis after hepatectomy for hepatocellular carcinoma on cirrhosis. Liver Transpl 12:966–971
5. Kamath PS, Kim WR, Advanced Liver Disease Study Group (2007) The model for end-stage liver disease (MELD). Hepatology 45:797–805
6. Tam HH, Collins DJ, Wallace T, Brown G, Riddell A, Koh DM (2012) Segmental liver hyperintensity in malignant biliary obstruction on diffusion weighted MRI: associated MRI findings and relationship with serum alanine aminotransferase levels. Br J Radiol 85:22–28
7. Watanabe H, Kanematsu M, Goshima S et al (2011) Staging hepatic fibrosis: comparison of gadoxetate disodium-enhanced and diffusion-weighted MR imaging—preliminary observations. Radiology 259:142–150
8. Verloh N, Haimerl M, Zeman F et al (2014) Assessing liver function by liver enhancement during the hepatobiliary phase with Gd-EOB-DTPA-enhanced MRI at 3 Tesla. Eur Radiol 24:1013–1019
9. Utsunomiya T, Shimada M, Hanaoka J et al (2012) Possible utility of MRI using Gd-EOB-DTPA for estimating liver functional reserve. J Gastroenterol 47:470–476
10. Saito K, Ledsam J, Sourbron S et al (2014) Measuring hepatic functional reserve using low temporal resolution Gd-EOB-DTPA dynamic contrast-enhanced MRI: a preliminary study comparing galactosyl human serum albumin scintigraphy with indocyanine green retention. Eur Radiol 24:112–119
11. Saito S, Moriyama Y, Kobayashi S et al (2012) Assessment of liver function in thioacetamide-induced rat acute liver injury using an empirical mathematical model and dynamic contrast-enhanced MRI with Gd-EOB-DTPA. J Magn Reson Imaging 36:1483–1489
12. Kim SU, Kim YC, Choi JS et al (2010) Can preoperative diffusion-weighted MRI predict postoperative hepatic insufficiency after curative resection of HBV-related hepatocellular carcinoma? A pilot study. Magn Reson Imaging 28:802–811
13. Materne R, Smith AM, Peeters F et al (2002) Assessment of hepatic perfusion parameters with dynamic MRI. Magn Reson Med 47:135–142
14. Ding Y, Rao SX, Meng T, Chen C, Li R, Zeng MS (2014) Usefulness of T1 mapping on Gd-EOB-DTPA-enhanced MR imaging in assessment of non-alcoholic fatty liver disease. Eur Radiol 24:959–966
15. Katsube T, Okada M, Kumano S et al (2011) Estimation of liver function using T1 mapping on Gd-EOB-DTPA-enhanced magnetic resonance imaging. Investig Radiol 46:277–283
16. Haimerl M, Verloh N, Zeman F et al (2013) Assessment of clinical signs of liver cirrhosis using T1 mapping on Gd-EOB-DTPA-enhanced 3 T MRI. PLoS One 8:e85658
17. Bruix J, Sherman M, Practice Guidelines Committee, American Association for the Study of Liver Diseases (2005) Management of hepatocellular carcinoma. Hepatology 42:1208–1236
18. Saito K, Araki Y, Park J et al (2010) Effect of Gd-EOB-DTPA on T2-weighted and diffusion-weighted images for the diagnosis of hepatocellular carcinoma. J Magn Reson Imaging 32:229–234
19. Choi JS, Kim MJ, Choi JY et al (2010) Diffusion-weighted MR imaging of liver on 3.0-Tesla system: effect of intravenous administration of gadoxetic acid disodium. Eur Radiol 20:1052–1060
20. Muhi A, Ichikawa T, Motosugi U et al (2012) Diffusion- and T2-weighted MR imaging of the liver: effect of intravenous administration of gadoxetic acid disodium. Magn Reson Med Sci 11:185–191
21. Van Beers BE, Pastor CM, Hussain HK (2012) Primovist, Eovist: what to expect? J Hepatol 57:421–429
22. Reimer P, Schneider G, Schima W (2004) Hepatobiliary contrast agents for contrast-enhanced MRI of the liver: properties, clinical development and applications. Eur Radiol 14:559–578
23. Lee JM, Zech CJ, Bolondi L et al (2011) Consensus report of the 4th international forum for gadolinium-ethoxybenzyl-diethylenetriamine pentaacetic acid magnetic resonance imaging. Korean J Radiol 12:403–415
24. Kitao A, Zen Y, Matsui O et al (2010) Hepatocellular carcinoma: signal intensity at gadoxetic acid-enhanced MR Imaging—correlation with molecular transporters and histopathologic features. Radiology 256:817–826
25. Bae KE, Kim SY, Lee SS et al (2012) Assessment of hepatic function with Gd-EOB-DTPA-enhanced hepatic MRI. Dig Dis 30:617–622
26. Yoshimura N, Saito K, Saguchi T et al (2013) Distinguishing hepatic hemangiomas from metastatic tumors using T1 mapping on gadoxetic-acid-enhanced MRI. Magn Reson Imaging 31:23–27
27. Erturk SM, Alberich-Bayarri A, Herrmann KA, Marti-Bonmati L, Ros PR (2009) Use of 3.0-T MR imaging for evaluation of the abdomen. Radiographics 29:1547–1563
28. de Bazelaire CM, Duhamel GD, Rofsky NM, Alsop DC (2004) MR imaging relaxation times of abdominal and pelvic tissues measured in vivo at 3.0 T: preliminary results. Radiology 230:652–659
29. Yamada A, Hara T, Li F et al (2011) Quantitative evaluation of liver function with use of gadoxetate disodium-enhanced MR imaging. Radiology 260:727–733
30. Tamada T, Ito K, Yamamoto A et al (2013) Simple Method for evaluating the degree of liver parenchymal enhancement in the hepatobiliary phase of gadoxetic acid-enhanced magnetic resonance imaging. J Magn Reson Imaging 37:1115–1121